Am J Transl Res 2014;6(3):206-223
www.ajtr.org /ISSN:1943-8141/AJTR0000294

Original Article

HDAC inhibitors mitigate ischemia-induced oligodendrocyte damage: potential roles of oligodendrogenesis, VEGF, and anti-inflammation

Hyeon Ju Kim, De-Maw Chuang

Molecular Neurobiology Section, National Institute of Mental Health, National Institutes of Health, Bethesda, MD 20892-1363, USA

Received March 21, 2014; Accepted April 18, 2014; Epub May 15, 2014; Published May 30, 2014

Abstract: White matter injury is an important component of stroke pathology, but its pathophysiology and potential treatment remain relatively elusive and underexplored. We previously reported that after permanent middle cerebral artery occlusion (pMCAO), sodium butyrate (SB) and trichostatin A (TSA) induced neurogenesis via histone deacetylase (HDAC) inhibition in multiple ischemic brain regions in rats; these effects-which depended on activation of brain-derived neurotrophic factor (BDNF)-TrkB signaling-contributed to behavioral improvement. The present study found that SB or TSA robustly protected against ischemia-induced loss of oligodendrocytes detected by confocal microscopy of myelin basic protein (MBP) immunostaining in the ipsilateral subventricular zone (SVZ), striatum, corpus callosum, and frontal cortex seven days post-pMCAO. Co-localization of 5-bromo-2'-deoxyuridine $(BrdU)^+$ and MBP^+ cells after SB treatment suggested the occurrence of oligodendrogenesis. SB also strongly upregulated vascular endothelial growth factor (VEGF), which plays a major role in neurogenesis, angiogenesis, and functional recovery after stroke. These SB-induced effects were markedly suppressed by blocking the TrkB signaling pathway with K252a. pMCAO-induced activation of microglia ($OX42^+$) and macrophages/monocytes ($ED1^+$)-which has been linked to white matter injury-was robustly suppressed by SB in a K252a-sensitive manner. In addition, SB treatment largely blocked caspase-3^+ and $OX42^+$ cells in ipsilateral brain regions. Our results suggest that HDAC inhibitor-mediated protection against ischemia-induced oligodendrocyte loss may involve multiple mechanisms including oligodendrogenesis, VEGF upregulation, anti-inflammation, and caspase-3 downregulation. Taken together, the results suggest that post-insult treatment with HDAC inhibitors is a rational strategy to mitigate white matter injury following ischemic stroke.

Keywords: Anti-inflammation, cerebral ischemia, HDAC inhibitors, myelin basic protein (MBP), oligodendrocytes, vascular endothelial growth factor (VEGF)

Introduction

Most stroke conditions stem from cerebral artery occlusions that block blood flow to the brain. The evolution of this ischemic pathophysiology is complex, and takes place within minutes to hours and over days. Extremely short-term events include energy depletion, excitotoxicity, calcium overload, and necrosis. Long-term events include apoptosis, cerebral infarction, oxidative stress, neuroinflammation, edema, and blood-brain barrier disruption [1].

Recent preclinical studies have identified histone deacetylase (HDAC) inhibitors as potential therapeutic drugs for a variety of brain disorders, including stroke (for a review, see [1-4]). Specifically, pan-HDAC inhibitors such as valproic acid (VPA), sodium butyrate (SB), and trichostatin A (TSA) have been found to decrease brain infarct volume, suppress neuroinflammation in the ischemic region, and reduce neurological deficits in a rat ischemic model using middle cerebral artery occlusion (MCAO) [5-7]. VPA and SB also repaired MCAO-induced disruption of the blood-brain barrier and reduced edema, at least partly by inhibiting NF-κB activation as well as matrix metalloproteinase expression and activity [8]. VPA also enhanced MCAO-induced angiogenesis by upregulating vascular endothelial growth factor

(VEGF) and other pro-angiogenic factors [8]. Furthermore, SB or TSA treatment via HDAC inhibition induced cell proliferation and neurogenesis in neurogenic niches such as the subventricular zone (SVZ) and dentate gyrus (DG), as well as in ischemic brain areas such as cortex and striatum [9]. In the latter study, SB-induced neurogenesis and behavioral improvement depended on BDNF-TrkB (the high-affinity receptor for BDNF) signaling pathway, in that intracerebral injection of K252a, a TrkB inhibitor, blocked all of these SB-induced beneficial effects.

Oligodendrocytes play a key role in the myelination of axons and contribute to the mechanisms of demyelination repair in the white matter region of the CNS [10, 11]. Oligodendrocytes are vulnerable to cerebral ischemia, resulting in depletion of the oligodendrocyte pool and white matter hypomyelination [12-14]. Injury to oligodendrocytes and white matter is key to the impaired brain function associated with a variety of pathological conditions, including stroke. N-methyl D-aspartate (NMDA) receptors with unusual subunit compositions were found to be expressed in oligodendrocytes and activated during ischemia, which triggered calcium overflow and excitotoxicity [15, 16]. Microglia activation is also thought to be an important mechanism for damaging oligodendrocyte precursor cells (OPCs)/oligodendrocytes under hypoxic/ischemic conditions by releasing pro-inflammatory factors [17-19]. Thus, oligodendrocytes and their progenitors are rational targets for therapeutic intervention to combat white matter injury after ischemic stroke.

Neural stem cells in the SVZ have the potential to produce new neurons and oligodendrocytes under both normal and pathological conditions [20, 21]. OPCs produced from restricted germinal zones including the SVZ can also migrate into the olfactory bulb, corpus callosum, and other white matter brain regions and subsequently differentiate into mature oligodendrocytes in the mammalian brain [22, 23]. Glia precursors originating in the SVZ also differentiate into oligodendrocytes and are involved in the myelination process [20, 24]. Exogenous BDNF and other neurotrophins have been shown to enhance oligodendrocyte proliferation and myelination, while inhibition of endogenous BDNF-TrkB signaling impairs myelination and regeneration in rodent injury models [25-27]. It has also been suggested that cerebral endothelial cells may secrete BDNF, which would in turn stimulate the survival and proliferation of oligodendrocytes, and promote myelination and remyelination [28]. Compared to our understanding of the mechanisms of ischemia-induced neuronal injury and protection in gray matter, white matter pathophysiology remains relatively elusive, as does the development of potential protective agents for oligodendrocyte damage. The present study was undertaken to investigate whether post-ischemic treatment with HDAC inhibitors-most notably SB-restores the loss of oligodendrocytes following permanent MCAO (pMCAO), and to explore the potential roles of oligodendrogenesis, VEGF upregulation, and anti-inflammation in protection against white matter injury.

Materials and methods

Animal model of focal cerebral ischemia

All experiments were approved by the Animal Care and Use Committee of the National Institutes of Mental Health (NIMH-NIH). Male Sprague Dawley rats (Charles River Laboratories, Charles River, CA) weighing 250-300 grams were anesthetized with 3% isoflurane in a 70% to 30% mixture of N_2O to O_2 and underwent permanent middle cerebral artery occlusion (pMCAO) as previously described [6, 9]. Briefly, the left common carotid artery and external carotid artery were isolated and ligated with a 4-0 suture. A nylon thread coated with silicon was inserted into the left internal carotid artery through a small puncture in the common carotid artery and advanced 17-18 mm past the carotid bifurcation to obstruct the origin of the middle cerebral artery. The thread was left in place until the rats were sacrificed, normally at Day 7 post-ischemia. Sham-operated control surgery was performed in an identical manner without insertion of the thread. Rectal temperature was maintained at 37 ± 0.5°C using a homoeothermic blanket.

Drug and BrdU administration

Rats received daily subcutaneous injections of either SB (300 mg/kg in 0.9% saline), TSA (0.2 mg/kg in DMSO) (both from Sigma, St. Louis, MO), or vehicle for seven days, starting immediately after pMCAO. Doses for the HDAC inhibitors were selected from our previous studies [6,

9]. 5-bromo-2'-deoxyuridine (BrdU), a thymidine analogue that is incorporated into DNA during the S phase of cell division [29], was used to characterize cell proliferation. Rats were intraperitoneally injected with BrdU (50 mg/kg in 0.9% saline, Sigma, St. Louis, MO) twice daily, from Days 3 to 7 after ischemia, and sacrificed on Day 7. This time point was chosen from prior studies that showed a maximal increase in SVZ cell proliferation after focal ischemia [9, 30].

Stereotaxic surgery and K252a treatment

Stereotaxic surgery for K252a micro-infusion was performed two hours before pMCAO. Rats were anesthetized by inhaling a mixture of 3% isoflurane, 70% N_2O, and 30% O_2 and then placed on a stereotaxic surgery apparatus (David Kopf Instruments, Tujunga, CA). The scalp was incised, and a small hole was made by drilling through the left skull. A Hamilton syringe needle (Hamilton, Reno, NV) was inserted into the left lateral ventricle (coordinates from the bregma: anterior-posterior-0.3 mm, medio-lateral (left) -1.2 mm, and dorsoventral -3.6 mm from the meninges). Five μl of K252a (0.5 mM dissolved in 1% DMSO, Sigma, MO, USA), a BDNF-TrkB receptor blocker, was injected into the left lateral ventricle by a Hamilton syringe at a rate of 1 μl/min. The dose of K252a was selected based on previous studies [9, 31]. The needle was left in place for two more minutes to allow for diffusion of the drug solution. Upon removal, the hole was cemented with bone wax. Rat body temperature was regulated with a heating pad during surgery. Typically, the experimental groups consisted of 1) vehicle (1% DMSO with pMCAO), 2) sham-operated (1% DMSO with sham), 3) SB-treated (1% DMSO + 300 mg/kg SB with pMCAO), 4) K252a-treated (K252a with pMCAO), and 5) K252a + SB-treated (K252a + 300 mg/kg SB with pMCAO). Each group comprised four to six animals for various immunohistochemical analyses to characterize cell phenotypes.

Immunohistochemistry

Rats were sacrificed by CO_2 exposure, and then transcardially perfused with phosphate-buffered saline (PBS) (pH, 7.4). All brain tissues were immediately immersed in dry ice-precooled isopentane and stored in a -80°C freezer. Coronal brain sections (20 μm) [corresponding, bregma -3.0 to -1.2 mm (SVZ) and bregma -4.52 to -3.14 (DG)] were cut with a cryostat and fixed with 4% p-formaldehyde. To detect newly generated $BrdU^+$ cells, brain sections were treated with 2 N HCl for 30 minutes to denature DNA, and slides were rinsed with a borate buffer (pH 8.4) for neutralization. Brain sections were incubated with 10% normal serum in the presence of 0.2% Triton X-100 for one hour at room temperature followed by incubation with primary antibodies overnight at 4°C. Primary antibodies used were as follows: rat anti-rat BrdU (1:100; Accurate Chemicals, Westbury, NY), rabbit anti-myelin basic protein (MBP) (1:200; Millipore, Temecula, CA), mouse anti-vascular endothelial growth factor (VEGF) (1:200; Millipore), mouse anti-ED1 for monocyte/macrophage (1:100; Serotec, Raleigh, NC), mouse anti-OX42 (CR3 complement receptor) for microglia (1:100; Serotec), and rabbit anti-cleaved caspase-3 (1:200; Cell Signaling Technology, Beverly, MA). Brain sections were rinsed three times with PBS (0.1 M, pH 7.4) containing 1% Triton X-100 (PBST), and then incubated at room temperature for one hour with Alexa Flour 555 anti-rat IgG (1:3000; Invitrogen, Eugene, Oregon), FITC-conjugated anti-mouse IgG, (1:100; Jackson Immunoresearch, West Grove, PA), FITC-conjugated anti-rabbit IgG (1:200; Jackson Immunoresearch), or Cy3-conjugated anti-rabbit IgG (1:200; Jackson Immunoresearch). Sections were further rinsed three times with PBST and mounted with Fluorescent Mounting Medium (Vector Laboratories, Inc., Buringame, CA). To verify the specificity of the immuno-labeling, various primary antibodies were omitted from the staining process as negative controls.

Confocal microscopy

Double immunoflourescence and images were obtained with a confocal laser-scanning microscope (LSM 510, Carl Zeiss, Oberkochen, Germany). Fluorescent images were acquired sequentially for red and green channels using excitation wavelengths of 543 nm (helium/neon, red Cy3-immunofluorescence) and 488 nm (argon, yellow-green Cy2-immunofluorescence), respectively. Single optical images or *z* series stacks of 0.5 to 2 μm slice thickness were used for confocal laser microscopy. Image analysis was performed using LSM 510 Imaging Browser and Adobe Photoshop (Adobe Systems, Mountain View, CA).

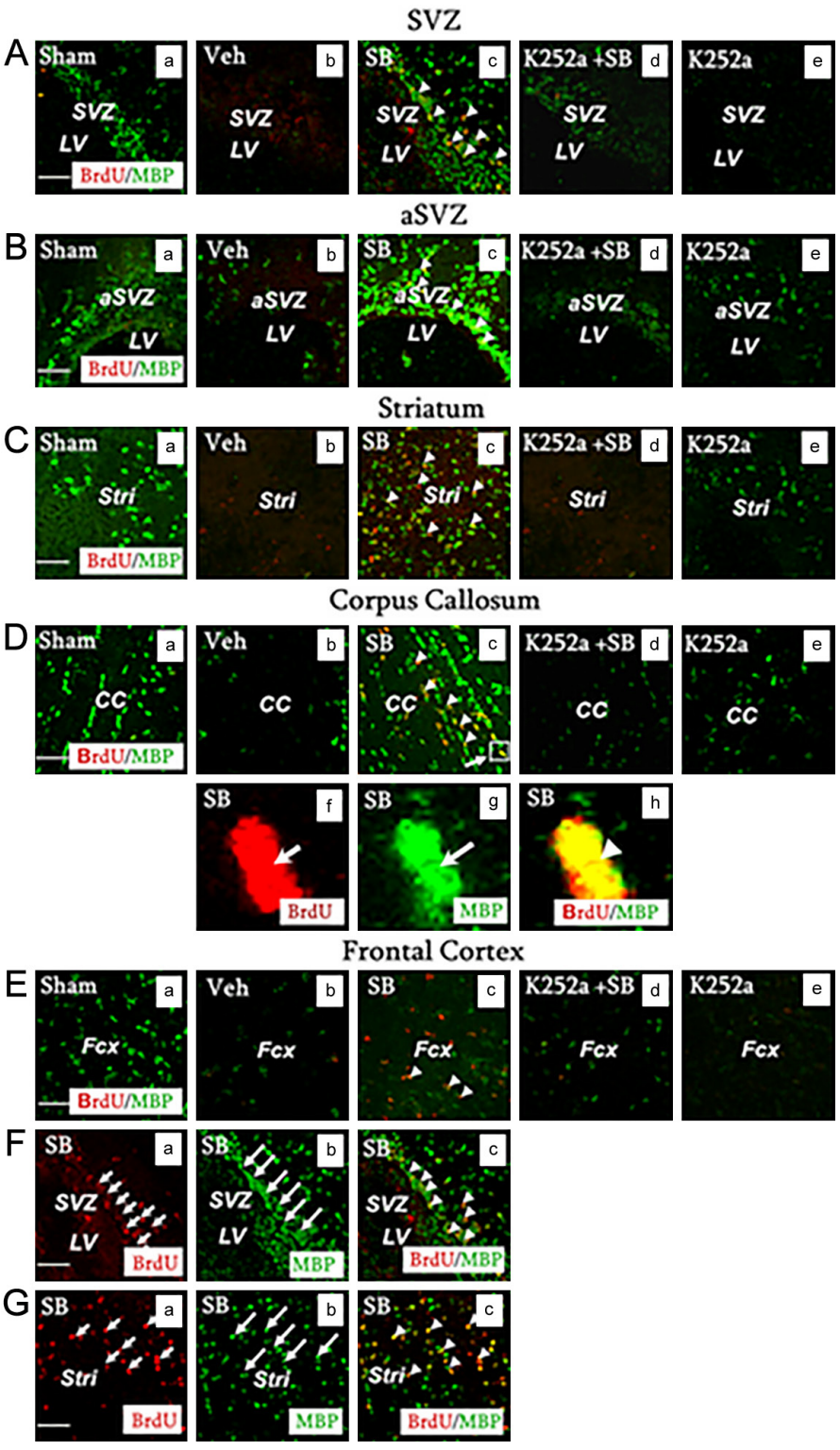

Figure 1. Post-insult sodium butyrate (SB) treatment increased 5-bromo-2'-deoxyuridine (BrdU)$^+$ and myelin basic protein (MBP)$^+$ cells in ipsilateral brain regions after permanent middle cerebral artery occlusion (pMCAO), and brain derived neurotrophic factor (BDNF)-TrkB inhibition by K252a blocked these increases. Animals were divided into five treatment conditions (n = 4-6 per group): (a) Sham, (b) Vehicle, (c) SB, (d) K252a + SB, and (e) K252a. On Day 7, brain sections were analyzed by immunostaining with BrdU (red)

Quantification of immunoreactive cells

Corresponding brain coronal sections including the SVZ, anterior SVZ (aSVZ), DG, frontal cortex, and striatum were selected for quantification using a rat atlas. In the SVZ and other brain areas, measurements were made using three to five sections per rat and four to six animals per group. Immunostaining for MBP$^+$, BrdU$^+$/VEGF$^+$, ED1$^+$, and OX42$^+$ cells by SB or TSA were quantified in the ipsilateral SVZ, aSVZ, striatum, corpus callosum (CC), and frontal cortex. Quantified results were obtained by confocal microscopy with a 40x objective lens within a square (225 μm × 225 μm). Analysis of BrdU and double-labeled cells in the ipsilateral SVZ and other brain regions was made using confocal *z*-series stacks. The phenotypes of newborn cells were identified via their double labeling with BrdU$^+$/MBP$^+$ and BrdU$^+$/VEGF$^+$. The number of cells expressing of single or double labeling were quantified. Images were analyzed using a Fiji software

and/or MBP (green) using confocal microscopy in multiple brain regions including (A) the subventricular zone (SVZ), (B) the anterior SVZ (aSVZ), (C) the striatum (Stri), (D) the corpus callosum, and (E) the frontal cortex. Merged images showed that BrdU$^+$ cells (arrows) and MBP$^+$ cells (longer arrows) co-localized (yellow indicated by arrowheads) in (Df-h) the corpus callosum, (Fa-c) the SVZ, and (Ga-c) the striatum of SB-treated pMCAO rats. Scale bar = 50 μm. Results are typical immunostainings from each experimental condition. Note that SB treatment markedly increased MBP and BrdU labeling with extensive co-localization, and that K252a treatment largely blocked these increases.

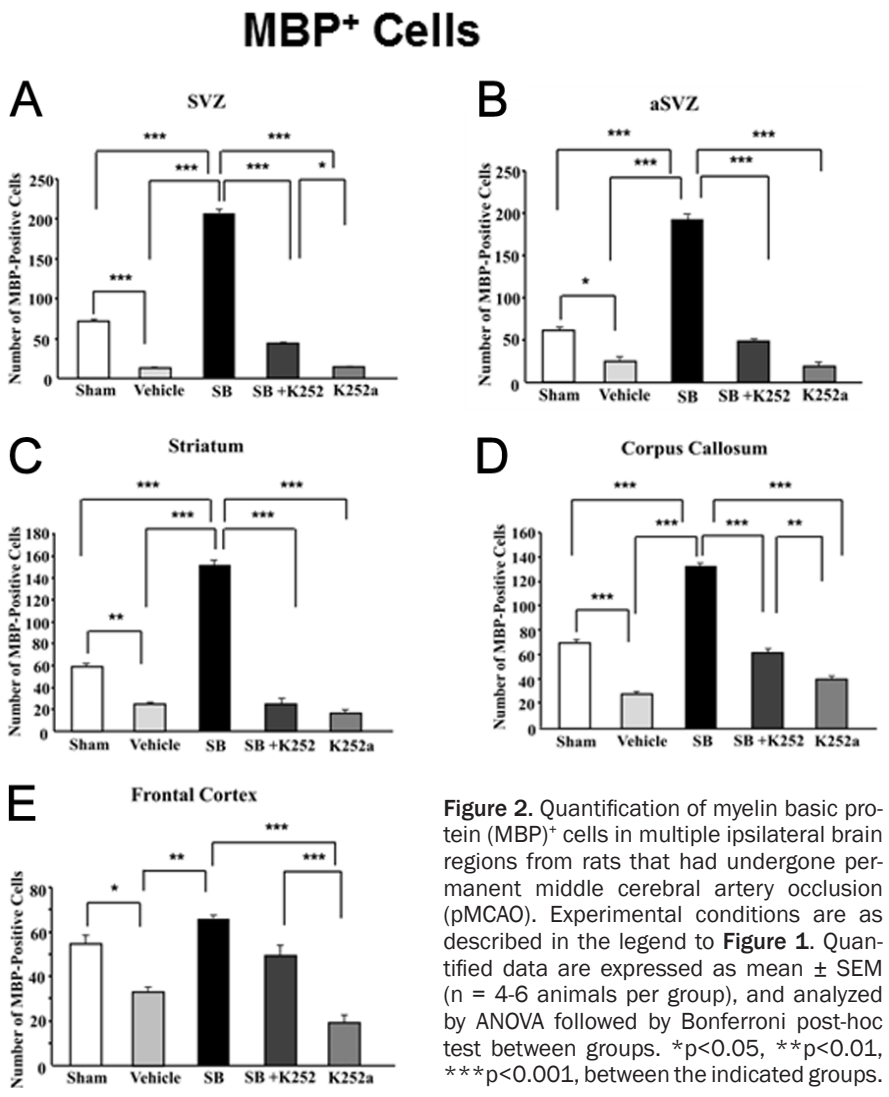

Figure 2. Quantification of myelin basic protein (MBP)$^+$ cells in multiple ipsilateral brain regions from rats that had undergone permanent middle cerebral artery occlusion (pMCAO). Experimental conditions are as described in the legend to **Figure 1**. Quantified data are expressed as mean ± SEM (n = 4-6 animals per group), and analyzed by ANOVA followed by Bonferroni post-hoc test between groups. *p<0.05, **p<0.01, ***p<0.001, between the indicated groups.

program adjusted for the threshold color value. Results were presented as the number of cells per section; significance was analyzed using Graph Pad Software (Prism 6, Graph Pad Inc., La Jolla, CA, USA).

Statistical analysis

Data are expressed as mean ± SEM. Differences between groups were measured using analysis of variance followed by post-hoc Bonferroni tests. Comparisons between two groups were performed using an unpaired Student's *t*-test. P<0.05 was considered statistically significant.

Results

Post-insult treatment with the HDAC inhibitors SB or TSA protected against pMCAO-induced loss of oligodendrocytes and stimulated oligodendrogenesis

Rats were subjected to permanent MCAO (pMCAO) followed by twice-daily injections of a cell proliferation marker BrdU (50 mg/kg, *i.p.)* from day 3 to 7 after ischemia. Where indicated, a TrkB antagonist K252a was injected into the lateral ventricle 2 h before MCAO and an HDAC inhibitor SB (300 mg/kg) or TSA (0.2 mg/kg) was administered once-daily, commencing immediately after ischemic onset. Immunohistochemical analyses were performed by confocal microscopy on Day 7 after the onset of pMCAO.

To address the question of whether SB could protect against the death of MBP-expressing oligodendrocytes and OPCs in the ischemic hemisphere, we examined the BrdU$^+$/MBP$^+$ cells in the SVZ and white matter regions of sham-operated versus vehicle-, SB-, K252a + SB-, and K252a-treated pMCAO rats. The vehi-

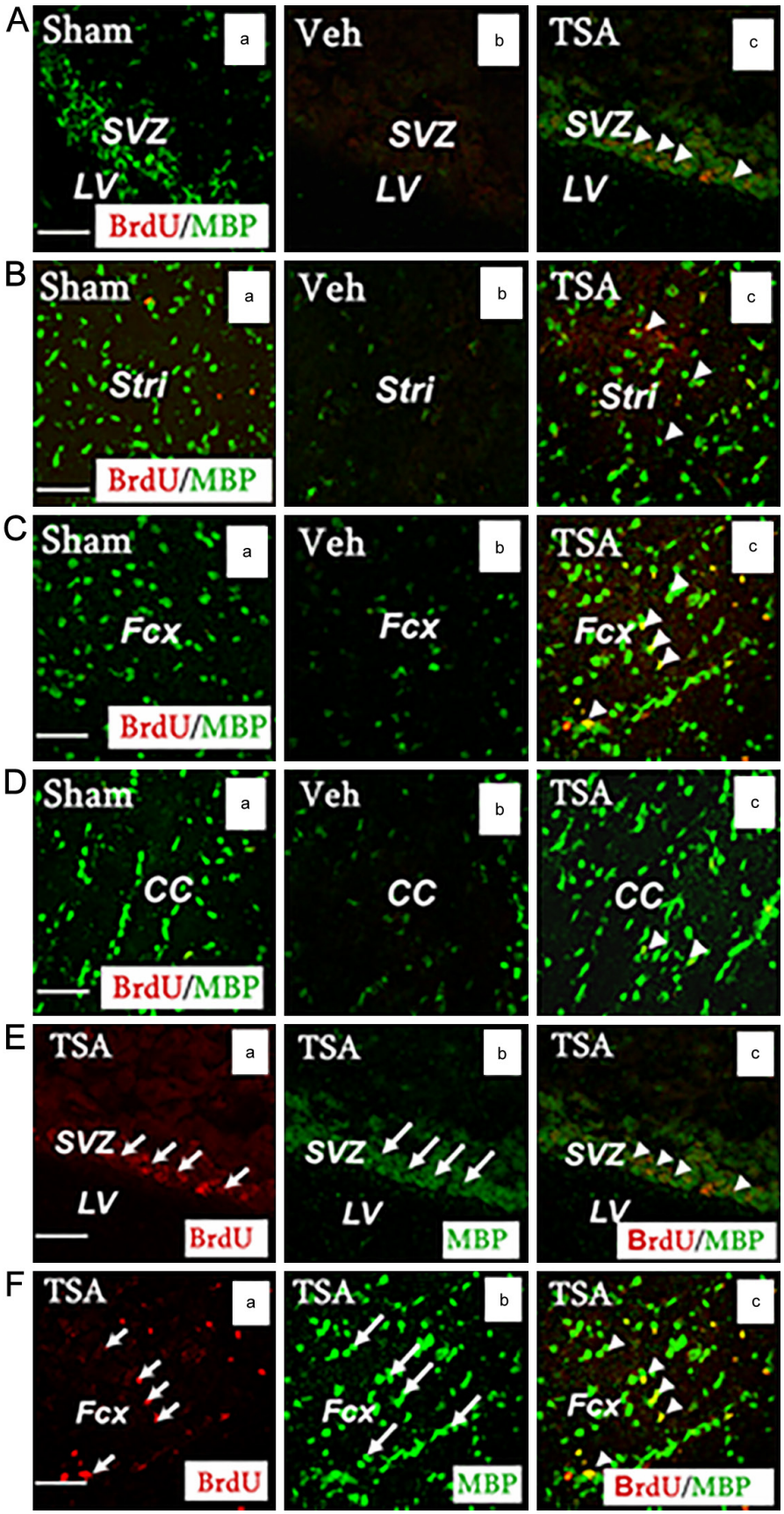

Figure 3. Post-insult trichostatin A (TSA) treatment increased labeling of 5-bromo-2'-deoxyuridine (BrdU)$^+$ and myelin basic protein (MBP)$^+$ immunostaining in the ipsilateral hemispheres on Day 7 after permanent middle cerebral artery occlusion (pMCAO). Sham or pMCAO rats treated with vehicle or TSA were examined for BrdU$^+$/MBP$^+$ immunostaining in (A) the subventricular zone (SVZ), (B) the striatum, (C) the frontal cortex, and (D) the corpus callosum. Note that TSA treatment enhanced BrdU$^+$ (red) and MBP$^+$ (green) labeling in all four brain regions, compared with vehicle treatment. Some co-localization of BrdU$^+$ and MBP$^+$ cells was observed, as indicated by arrowheads (yellow) in (E) the SVZ and (F) the frontal cortex; merged images further confirmed BrdU (arrow) and MBP (longer arrow) co-localization (arrowhead) after TSA treatment. Scale bar = 50 μm. Results are typical immunostainings from each experimental group.

cle-treated pMCAO group showed decreased labeling of MBP$^+$ cells in the ipsilateral SVZ, anterior SVZ (aSVZ), striatum, corpus callosum, and frontal cortex at 7 days after ischemic onset (**Figure 1Ab-Eb**), in contrast to the corresponding brain areas of the sham-operated animals (**Figure 1Aa-Ea**). No-

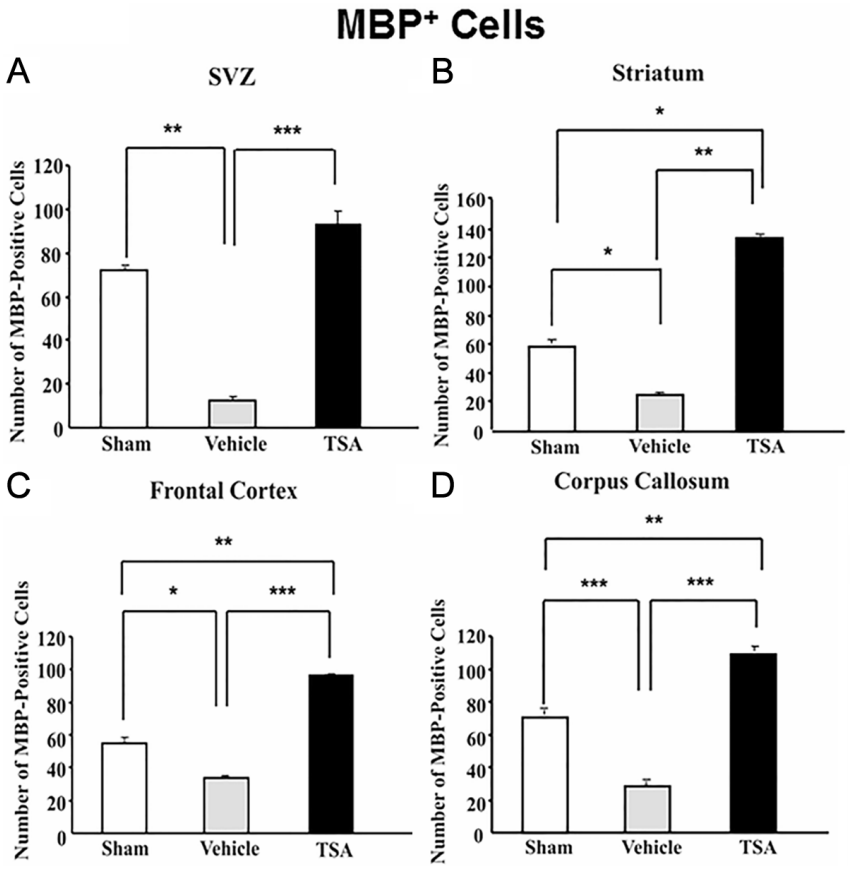

Figure 4. Quantification of myelin basic protein (MBP)$^+$ cells in the ipsilateral brain regions of sham, vehicle-, and TSA-treated rats that underwent permanent middle cerebral artery occlusion (pMCAO). Experimental conditions are described in the legend to **Figure 3**. Quantified data of MBP$^+$ cells in (A) the subventricular zone (SVZ), (B) the striatum, (C) the frontal cortex, and (D) the corpus callosum are expressed as mean ± SEM (n = 4-6 animals per group) and analyzed by ANOVA followed by Bonferroni post-hoc test between groups. *p<0.05, **p<0.01, ***p<0.001, between the indicated groups.

tably, SB treatment robustly enhanced the labeling of MBP$^+$ cells in the ischemic SVZ, aSVZ, striatum, corpus callosum, and frontal cortex on Day 7 after pMCAO (**Figure 1Ac-Ec**). Merged images revealed extensive co-localization of BrdU and MBP immunoreactive cells in the corpus callosum, SVZ, and striatum after SB treatment (**Figure 1Df-h**, **1Fa-c** and **1Ga-c**), suggesting the occurrence of oligodendrogenesis. Pre-treatment with K252a, a TrkB antagonist, blocked SB-induced increases in BrdU$^+$/MBP$^+$ cell labeling in these multiple brain regions of the ischemic hemisphere (**Figure 1Ad-Ed**). Treatment with K252a alone had no apparent effect on the labeling of BrdU$^+$/MBP$^+$ cells in the ischemic brain regions compared with vehicle treatment (**Figure 1Ae-Ee**). Quantified results demonstrated that SB treatment significantly increased the number of MBP$^+$ cells by several fold in the ipsilateral SVZ, aSVZ, striatum, and corpus callosum compared to that of vehicle-treated pMCAO rats ($p<0.001$), and that K252a pre-treatment almost completely prevented these SB-induced increases (**Figure 2A-D**). Similar, but less robust effects were found for SB in the frontal cortex (**Figure 2E**). The qualified data also confirmed that pMCAO markedly reduced the number of MBP$^+$ cells in the ischemic regions, and that these effects were not significantly altered by treatment with K252a alone (**Figure 2A-E**).

Post-insult treatment with TSA also resulted in abundant labeling of BrdU$^+$/MBP$^+$ cells in the ischemic SVZ, striatum, frontal cortex, and corpus callosum (**Figure 3Ac-Dc**). Merged images of BrdU$^+$ and MBP$^+$ labeling showed their colocalization in the SVZ and frontal cortex after TSA treatment (**Figure 3Ea-c** and **3Fa-c**). Quantifying the number of MBP$^+$ cells showed that pMCAO-induced loss of MBP$^+$ cells in the SVZ, striatum, frontal cortex, and corpus callosum was restored to or above the levels of sham control after TSA treatment (**Figure 4A-D**). Because MBP is a marker of mature oligodendrocytes and late-stage oligodendrocyte progenitor cells [32-33], our results collectively support the critical role of HDAC inhibitors (SB and TSA) in protecting against ischemia-induced damage to oligodendrocytes. This protection may at least partly involve oligodendrogenesis by epigenetic mechanisms.

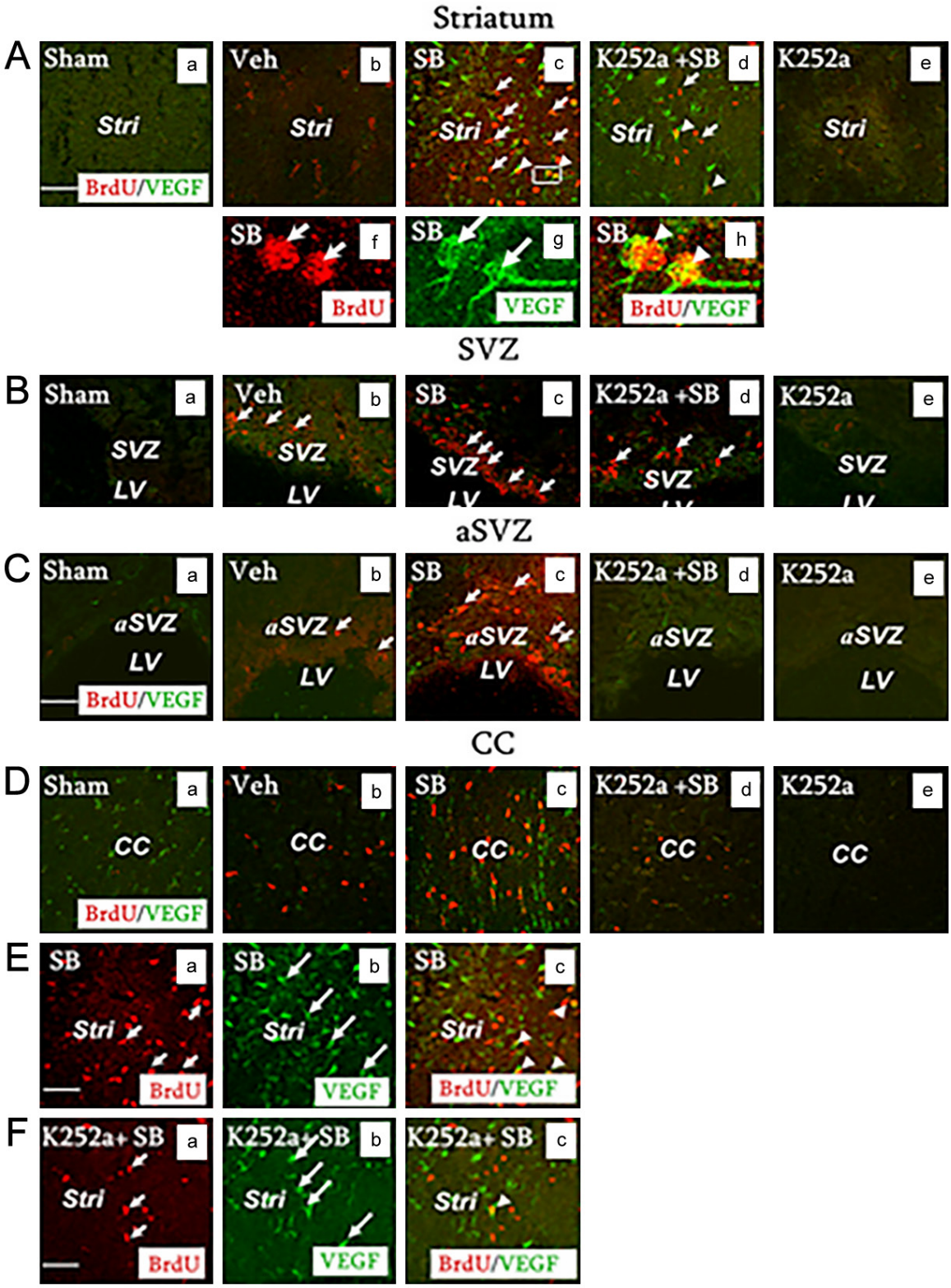

Figure 5. 5-bromo-2'-deoxyuridine (BrdU)$^+$ and vascular endothelial growth factor (VEGF)$^+$ cells in the ipsilateral brain regions of rats that underwent permanent middle cerebral artery occlusion (pMCAO) were upregulated by treatment with sodium butyrate (SB), and this effect was blocked by inhibiting brain derived neurotrophic factor (BDNF)-TrkB with K252a. Animals were divided into five treatment conditions (n = 4-6 per group): (a) Sham, (b) Vehicle, (c) SB, (d) K252a + SB, and (e) K252a. Brain sections were analyzed by immunostaining with BrdU (red) and/or VEGF (green)

in multiple brain regions including (A) the striatum, (B) the subventricular zone (SVZ), (C) the anterior SVZ (aSVZ), and (D) the corpus callosum. Note that SB treatment markedly enhanced $BrdU^+$ and $VEGF^+$ cell labeling in these brain regions with some co-localization, most notably in the striatum (Af-h). Pre-treatment with K252a suppressed these SB-induced changes in BrdU and VEGF labeling. Merged images in the striatum showed $BrdU^+$ (arrow) and $VEGF^+$ (longer arrow) co-localization (arrowhead) in (E) the SB and (F) the K252a + SB groups. Scale bar = 50 μm. Results are typical immunostainings from each experimental condition.

SB treatment increased $BrdU^+/VEGF^+$ cells in ischemic brain regions

VEGF plays a major role in angiogenesis, neurogenesis, cell protection, and functional recovery after cerebral ischemia [7, 34-37]. BDNF-dependent activation of TrkB was also found to induce VEGF in neuroblastoma cells [38]. We evaluated the effects of SB treatment on the expression of $BrdU^+$, $VEGF^+$, and $BrdU^+/VEGF^+$ cells. Sham-operated rats showed weak $BrdU^+$ and $VEGF^+$ labeling in the ischemic striatum, SVZ, aSVZ, and corpus callosum (**Figure 5Aa-Da**). Compared to vehicle treatment, SB robustly increased $BrdU^+$ and $VEGF^+$ labeling in the above-mentioned ischemic brain regions (**Figure 5Ac-Dc** v.s. **5Ab-Db**). Some colocalization of $BrdU^+$ and $VEGF^+$ labels were noted after SB treatment in these ischemic brain regions, notably in the striatum (**Figure 5Af-h** and **5Ea-c**). Pre-treatment with K252a suppressed the SB-induced increase in $BrdU^+$ and $VEGF^+$ labels in these brain regions (**Figure 5Ae-De** and **5Fa-c**). Quantification of the immunohistochemical results confirmed that SB dramatically increased the number of $BrdU^+$ or $VEGF^+$ cells in the ischemic striatum, SVZ, aSVZ, and corpus callosum, and that these increases were blocked by pre-treatment with K252a (**Figure 6A**, **6B**, **6D**, **6E**, **6G**, **6H**, **6J**, and **6K**). The number of $BrdU^+/VEGF^+$ cells was also markedly elevated by SB treatment in a K252a-sensitive manner in the striatum and corpus callosum and, to a lesser extent, in the SVZ and aSVZ (**Figure 6C**, **6F**, **6I**, and **6L**). In the vehicle-treated pMCAO group, the number of $BrdU^+$ cells was consistently increased in various brain regions (**Figure 6A**, **6D**, **6G** and **6J**), similar to our previous results [9]. However, the number of $VEGF^+$ or $BrdU^+/VEGF^+$ cells in the vehicle-treated group was more variable, and depended on the brain regions examined.

SB decreased pMCAO-induced inflammatory cells and caspase-3 activation

Cerebral ischemia is accompanied by acute and chronic inflammation that plays a critical role in the pathophysiology of stroke [39-41]. Activated microglia and infiltrating blood-derived cells such as monocytes/macrophages are key players in mediating pMCAO-induced neuroinflammation [6]. Activated microglia/macrophages surround the damaged axon bundles, contributing to white matter injury in the mouse brain after transient focal ischemia [19]. Therefore, we next examined ED1 and OX42 immunostaining in the ischemic brain seven days after pMCAO with and without SB treatment. ED1 is a cellular marker specific for monocytes/macrophages and activated microglia. When monocytes/macrophages are in resting or inactivated status, staining with their cellular antigen, ED1 is characterized by small, round cell bodies. None of the sham-operated animals expressed $ED1^+$ cells (**Figure 7Aa-Ca**); however, the vehicle-treated pMCAO group typically exhibited highly activated or reactive monocytes/macrophages with large round morphology in the ischemic striatum, frontal cortex, and parietal cortex (**Figure 7Ab-Cb**). On Day 7 after pMCAO, post-insult SB treatment reduced the immune staining of $ED1^+$ cells in all three ischemic brain regions compared with the vehicle group (**Figure 7Ac-Cc**). Quantified data confirmed a dramatic increase in the number of $ED1^+$ cells in the ischemic striatum, frontal cortex, and parietal cortex; these monocyte/macrophage recruitments were effectively blocked by SB treatment (**Figure 7D-F**).

OX42 (anti-CD11b) is a preferential marker of activated microglia, although it is also present in polymorphonuclear neutrophils (PMN) and macrophages [41-43]. Little or no staining of $OX42^+$ cells was observed in the brains of sham-operated animals (**Figure 8Aa** and **8Ba**). In contrast, strong staining of $OX42^+$ activated microglia was observed in vehicle-treated pMCAO rats; the staining was characterized by amoeboid-like morphology in the ipsilateral corpus callosum and frontal cortex seven days after ischemic onset (**Figure 8Ab** and **8Bb**). Post-insult SB treatment significantly decreased the number of $OX42^+$ cells compared to vehicle-treated control animals (**Figure 8Ac** and **8Bc**).

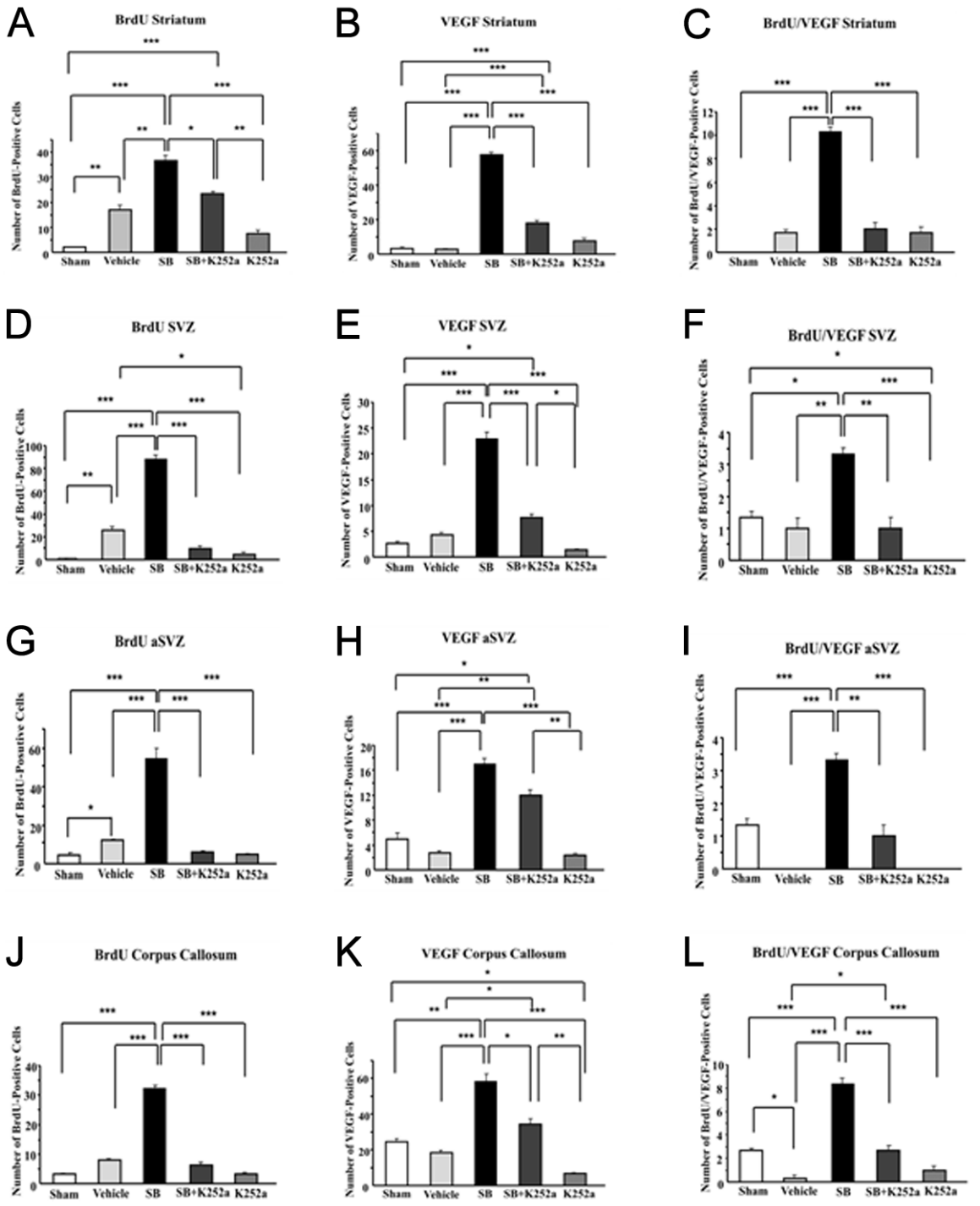

Figure 6. Quantification of 5-bromo-2'-deoxyuridine (BrdU)$^+$, vascular endothelial growth factor (VEGF)$^+$, and BrdU/VEGF$^+$ cells in ipsilateral brain regions of rats that underwent permanent middle cerebral artery occlusion (pMCAO). Experimental conditions are as described in the legend to **Figure 5**. Quantified data are expressed as mean ± SEM (n = 4-6 animals per group), and analyzed by ANOVA followed by Bonferroni post-hoc test between groups. *p<0.05, **p<0.01, ***p<0.001, between the indicated groups.

Pre-treatment with K252a alleviated the effects of SB on pMCAO-induced microglial activation, while pre-treatment with K252a alone appeared to enhance pMCAO-induced microglial activa-

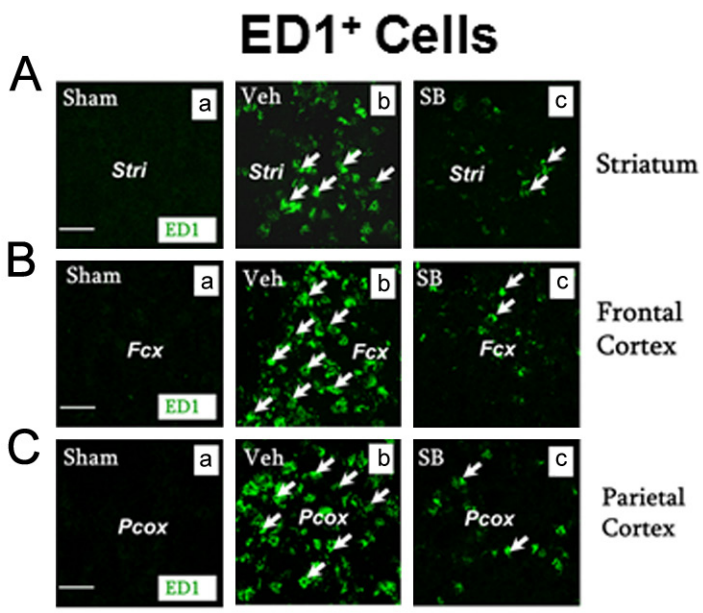

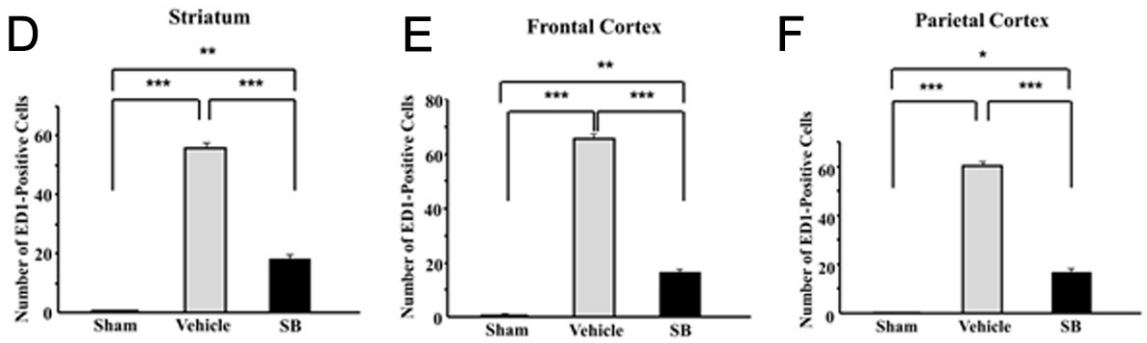

Figure 7. Confocal images of ED1+ cells in the ipsilateral brain regions seven days after permanent middle cerebral artery occlusion (pMCAO): the effects of post-insult treatment with sodium butyrate (SB). Animals were divided into three treatment conditions (n = 4-6 per group): (a) Sham, (b) Vehicle-, and (c) SB-treated. Brain sections were analyzed by immunostaining for ED1+ cells (green), as indicated by arrows, in (A) the striatum, (B) the frontal cortex, and (C) the parietal cortex. Scale bar = 50 μm. Quantified results of ED1+ cells in (D) the ipsilateral striatum, (E) the frontal cortex, and (F) the parietal cortex are expressed as mean ± SEM (n = 4-6), and analyzed by ANOVA followed by Bonferroni post-hoc tests between groups. *p<0.05, **p<0.01, ***p<0.001, between the indicated groups. Note that post-insult SB treatment effectively suppressed pMCAO-induced increases in ED1+ cells in all three brain regions.

tion (**Figure 8Ad**, **8Ae**, **8Bd** and **8Be**). Quantification of OX42+ cells in the corpus callosum and frontal cortex in various experimental groups confirmed the morphological assessments of OX42 immunostaining (**Figure 8C** and **8D**).

Activated microglia, macrophages, or monocytes produce and release highly toxic substances such as peroxynitrite, cytokines, and reactive oxygen species (ROS), which in turn trigger tissue damage and cell death [44]. On the other hand, ischemia–induced brain damage appears to involve mitochondrial dysfunction, cytochrome c release, and caspase-9/caspase-3 activation [45]. Caspase-3 functions as a central regulator of apoptosis, and caspase-3 inhibition robustly protects neurons against ischemia-induced cell death [46]. To investigate the link between caspase-3 activation and microglia, we performed double immunostaining of OX42+ and cleaved (activated) caspase-3+ in the ipsilateral brain regions. We found abundant OX42+ and caspase-3+ cells in the piriform cortex, corpus callosum, and striatum in the vehicle-treated pMCAO group seven days after ischemic onset (**Figure 9Ab-Cb**). SB treatment largely blocked ischemia-induced caspase-3 and OX42+ immunostaining in the ipsilateral brain regions; these protective effects were blocked by pre-treatment with K252a (**Figure 9Ac-e-Cc-e**). It is also noteworthy that after SB treatment, co-localization of caspase-3+ and OX42+ cells in the ischemic striatum still persisted, despite an overall reduction in surrounding caspase-3+ cells (**Figure 9Cc** and **9Da-c**). In contrast, the vehicle-treated pMCAO group showed no striatal co-localization of caspase-3+ and OX42+ cells (**Figure 9Ea-c**). K252a pre-treatment reversed SB-induced decreases in caspase-3+ and OX42+ immunostaining in the ipsilateral piriform cortex, corpus callosum, and striatum (**Figure 9Ad-Cd**).

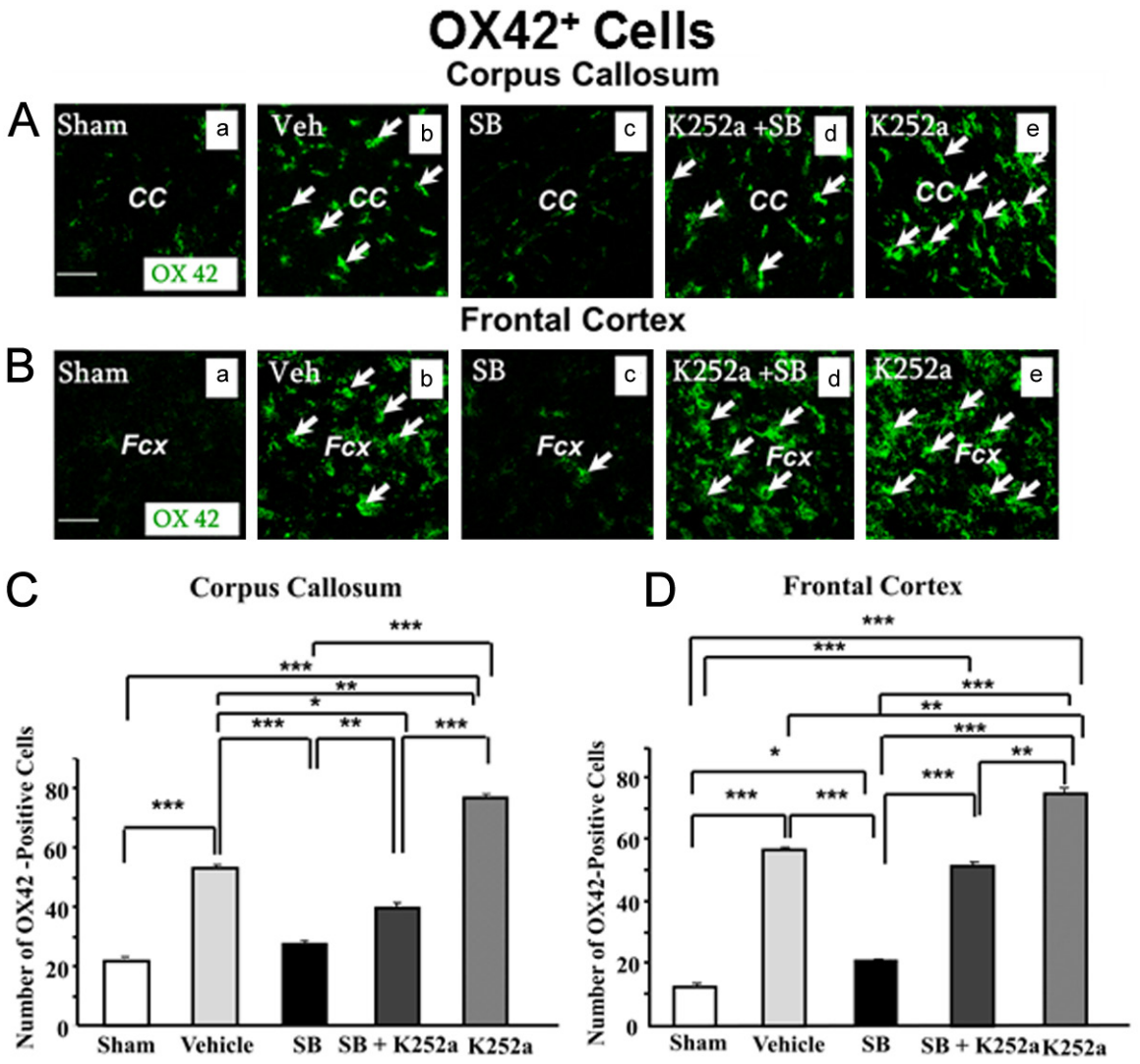

Figure 8. Treatment with sodium butyrate (SB) decreased OX42$^+$ cells in the ipsilateral brain regions after permanent middle cerebral artery occlusion (pMCAO). Animals were divided into five treatment conditions (n = 4-6 per group): (a) Sham, (b) Vehicle, (c) SB, (d) K252a + SB, and (e) K252a. Brain sections were analyzed by immunostaining for OX42$^+$ cells (green), as indicated by arrows, in the ipsilateral (A) corpus callosum and (B) frontal cortex. Scale bar = 50 μm. Quantified results of OX42$^+$ cells in (C) corpus callosum and (D) frontal cortex are expressed as mean ± SEM (n = 4-6 per group) and analyzed by ANOVA followed by Bonferroni post-hoc test between groups. *p<0.05, **p<0.01, ***p<0.001 between the indicated groups. Note that post-insult SB treatment markedly decreased pMCAO-induced increase in OX42$^+$ cells in both brain regions and that this SB effect was attenuated by K252 treatment. K252a alone induced a significant increase over the vehicle-treated group.

Discussion

This study demonstrated that pMCAO induced the loss of oligodendrocytes labeled by MBP$^+$, a marker of mature oligodendrocytes and late stage OPCs, in multiple brain regions including SVZ, aSVZ, striatum, corpus callosum, and frontal cortex. Remarkably, post-insult treatment with two structurally unrelated HDAC inhibitors, SB and TSA, robustly increased the number of MBP$^+$ cells in these brain regions to levels approximating those of sham-operated controls (**Figures 1**-**4**). The co-localization of BrdU$^+$/MBP$^+$ cells suggests that the protective effects of HDAC inhibition partly involve oligodendrogenesis. OPCs are normally located in the germinal zone of the SVZ, but can migrate to various brain regions after stroke or under other pathological conditions [20, 47, 48]. These observations could explain the diversity of pro-

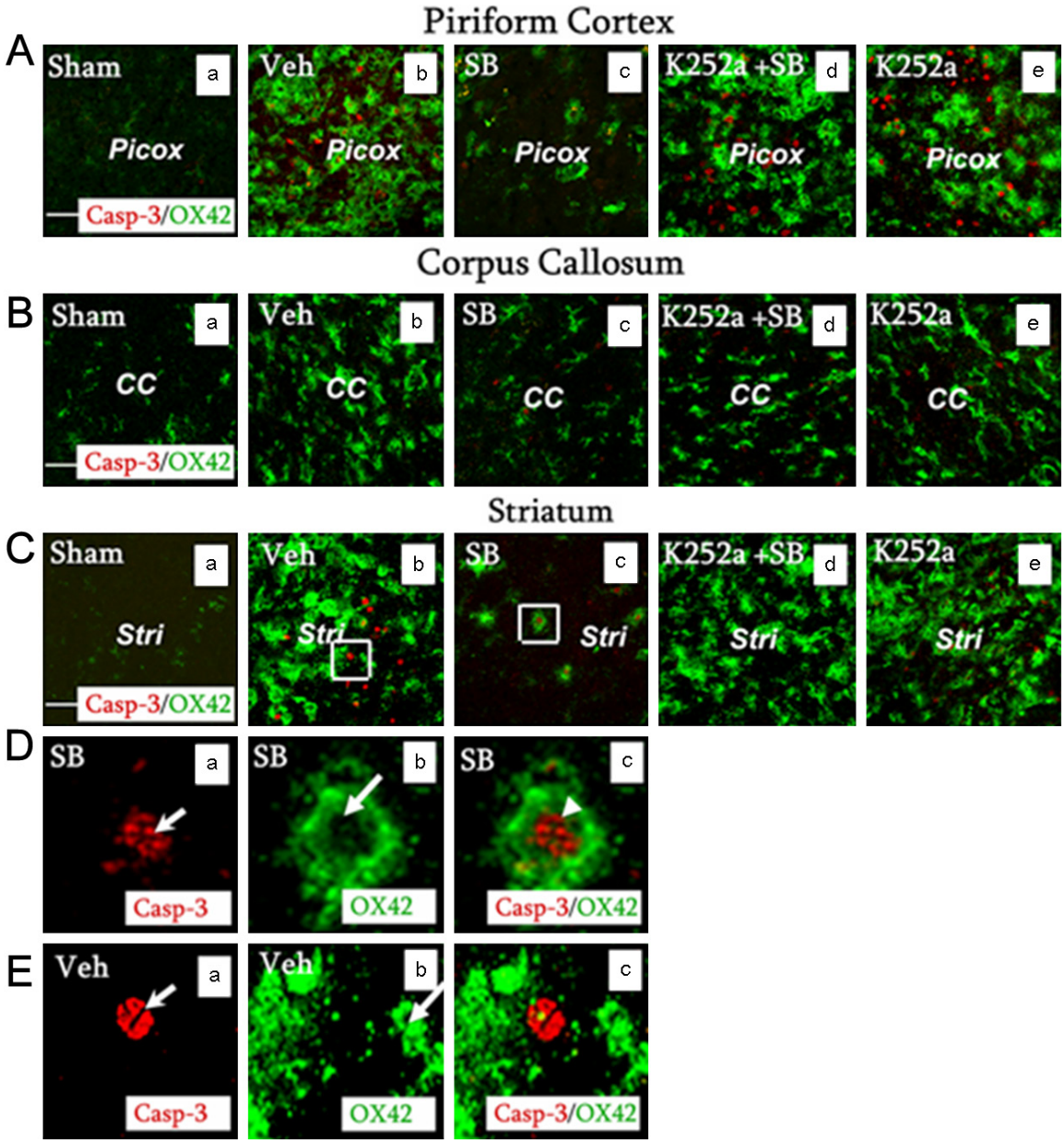

Figure 9. Treatment with sodium butyrate (SB) robustly suppressed ischemia-induced caspase-3 and/or OX42 immunoreactive cells in the ipsilateral brain regions in a K252a-sensitive manner. Animals were divided into five treatment conditions (n = 4-6 per group): (a) Sham, (b) Vehicle, (c) SB, (d) K252a + SB, and (e) K252a. On Day 7, brain sections were prepared and analyzed by immunostaining for caspase-3 (red) and/or OX42 (green) using confocal microscopy in (A) the piriform cortex, (B) the corpus callosum, and (C) the striatum. Scale bar = 50 μm. Results are typical immunostaining from each experimental condition. Note that SB treatment markedly reduced pMCAO-induced increases in caspase-3 and OX42-immunostaining, and these SB effects were sensitive to pre-treatment with K252a. Magnified, merged images from the boxes in (C) show that caspase-3 (arrows) and OX42 (longer arrows) were co-localized (arrowheads) in the striatum of the SB-treated group (Da-c), but no such co-localization was detected in the vehicle-treated group (Ea-c).

tective effects associated with HDAC inhibitors seen in multiple brain sites in our study. Consistent with this notion, a report found that delayed (24 hours) administration of VPA, a pan-HDAC inhibitor structurally similar to SB, increased oligodendrocyte survival and promoted OPC differentiation into mature oligodendrocytes in the ischemic rat brain 28 days

after pMCAO [49]. In addition, suberoyl anilide hydroxamic acid (SAHA) and the class I-specific HDAC inhibitor MS-275 were both found to preserve white matter cellular architecture. This protective effect correlated with reduced excitotoxicity, maintenance of ATP, and preservation of axonal mitochondria and oligodendrocytes during oxygen-glucose deprivation in a pure white matter tract of optic nerve [50, 51].

In the present study, the protective effects of SB against pMCAO-induced loss of oligodendrocytes were associated with the anti-inflammatory effect of this HDAC inhibitor. Specifically, SB treatment suppressed ischemia-induced microglial activation detected by OX42 immunostaining in the corpus callosum and frontal cortex (**Figure 8**) and by ED1$^+$ staining for macrophage/monocytes and macrophage in the striatum and frontal/parietal cortex (**Figure 7**). Peroxynitrite produced by iNOS and NAPDH oxidase in activated microglia have been shown to mediate the death of oligodendrocytes [52]. Our preliminary data showed that hypoxia/ischemia induced by unilateral common carotid ligation in mice increased the loss of MBP$^+$, ED1$^+$, and GFAP$^+$ cells in ischemic white matter as well as the CA3 region, suggesting that microglial activation contributes to oligodendrocyte death in neonatal periventricular leukomalacia (Kim et al., 2010, unpublished data, SFN abstract, 567.10). In further support of the role of neuroinflammation in white matter injury is that ED1$^+$ macrophages/microglia are located in the damaged, but not undamaged, axonal bundles after ischemic injury [19], and that minocycline treatment reduced OX42$^+$ immunoreactivity and prevented the loss of MBP$^+$ immunostaining in a rat model of cerebral hypoperfusion [53]. Taken together, the data suggest that HDAC inhibition-mediated suppression of microglial activation and macrophage/monocyte infiltration after ischemic stroke is likely to be another important mechanism for improving the survival of oligodendrocytes after ischemic stroke.

We previously reported that post-ischemic SB or VPA treatment super-induced heat shock protein 70 [6], which has been shown to suppress microglial/monocyte activation after experimental stroke [54]. In addition, these two HDAC inhibitors blocked MCAO-induced activation of NF-κB [8], which is a key molecule mediating neuroinflammation. It has been proposed that JNK signaling is the shared pathway linking neuroinflammation and oligodendroglial apoptosis in the immature brain [55]. Whether JNK is a treatment target for HDAC inhibitors to elicit protection against oligodendrocyte death remains to be studied.

A striking feature of the current study is that the protective effects of SB against oligodendrocyte loss and its ability to reduce pMCAO-induced OX42$^+$ and ED1$^+$ cells in multiple brain regions were robustly suppressed by intraventricular injection of K252a to inhibit TrkB (**Figures 1**, **2**, **8** and **9**). These results were reminiscent of our previous study, which found that SB-induced neurogenesis in the SVZ, striatum, frontal cortex, and other regions of the ischemic brain was largely blocked by K252a, and involved activation of the BDNF-TrkB signaling pathway [9]. That study also demonstrated that the effects of SB on neurogenesis were accompanied by upregulation of histone acetylation and BDNF as well as activation of a BDNF downstream signaling molecule, cAMP-response element-binding protein (CREB). Activation of CREB by Ser133 phosphorylation is part of the molecular mechanism underlying BDNF-TrkB-induced migration, differentiation, and survival of SVZ neuroblasts [56]. In addition, phospho-CREB is a prominent transcription factor involved in the expression of numerous neuroprotective, neurotrophic, and anti-inflammatory protein molecules (reviewed in [3]). It is conceivable that similar BDNF-TrkB-mediated signaling mechanisms may be involved in SB-induced oligodendrogenesis, oligodendrocyte protection, and neuroinflammation suppression in ischemic brain regions. The critical role of the BDNF-TrkB pathway in the protection by HDAC inhibitors after stroke is further supported by our observation that HDAC inhibition-mediated functional recovery after stroke was blocked by K252a [9]. It is noteworthy that thyroxin T4-induced protection against white matter injury in the immature brain was previously found to be BDNF-TrkB-dependent [57], and that a TrkB agonist had profound protective effects after perinatal hypoxia and ischemia in mice [58].

We also found that SB treatment increased VEGF$^+$ cells in the ischemic striatum, SVZ, aSVZ, and corpus callosum, with notable co-localization of BrdU$^+$/VEGF$^+$ cells in the striatum and corpus callosum; these effects were blocked by

K252a (**Figures 5** and **6**). Recent research has underscored the role of VEGF in angiogenesis, neurogenesis, brain protection, and functional recovery after experimental stroke [7, 34-37, 59]. For instance, blockade of VEGF receptor-2 worsened brain injury, promoted apoptotic cell death, and reduced endothelial cell proliferation after neonatal stroke in rodents [37]. In a previous study, we found that, two weeks after transient pMCAO, suppression of VPA-induced VEGF by pharmacological inhibition of HIF-1α prevented enhanced angiogenesis and functional recovery [7]. BDNF-stimulated increases in HIF-1α and VEGF require the activity of the TrkB tyrosine kinase, PI-3 kinase, and mTOR pathways [38]. Thus, it is not surprising that in our study, SB-induced VEGF$^+$ cells in various ischemic brain regions were blocked by K252a. Because cerebral endothelial cells secrete trophic factors to support the survival and proliferation of OPCs via Akt and Src-dependent mechanisms [60], it is possible that VEGF is one of the prominent growth factors secreted by endothelial cells to mediate these effects.

Intracerebral injection of BDNF was found to protect against hypoxia/ischemia-induced infarction and caspase-3 activation in neonatal brain via the BDNF-TrkB signaling pathway [61]. In the present study, the HDAC inhibitor SB markedly suppressed caspase-3$^+$ and OX42$^+$ immunostaining in the cortex, corpus callosum, and striatum, and these effects were blocked by K252a (**Figure 8**), suggesting a close relationship between microglia/macrophage activation and caspase-3-dependent cell death. Interestingly, some co-localization of caspase-3$^+$ and OX42$^+$ cells was noted in the ischemic brain region after SB treatment, despite a global reduction of caspase-3$^+$ and OX42$^+$ cells (**Figure 9Da-c**). This observation is in line with a previous study demonstrating that HDAC inhibitors, including SB, induced microglial apoptosis to protect against inflammation-triggered dopaminergic neuronal death [62]. It should be noted that caspases can exert both apoptotic and non-apoptotic actions in neuronal physiology and pathology [46]. For example, caspase-3 activation limited self-renewal without triggering apoptosis in neural progenitor cells after stroke [63]. Whether apoptosis-independent effects of caspase-3 are involved in the regulation of the OPC regenerative response and oligodendrocyte protection in the ischemic brain are currently unknown.

SB, VPA, TSA, and SAHA are broad-spectrum inhibitors of zinc-dependent HDACs that preferentially affect Class I (isoforms 1, 3, 5, 8), have less effects on Class IIa (isoforms 2, 4, 7, 9), and have little or no effects on Class IIb (isoforms 6, 10). Global HDAC inhibition has also been shown to partially reverse the lineage restriction of OPCs, thereby inducing developmental plasticity [64]. The HDAC isoform(s) involved in the protective effects on oligodendrocytes after ischemic stroke remains unidentified. In this context, inhibition or deletion of HDAC isoform 2 has been reported to suppress neurodegeneration and improve behavioral performance in animal models of Alzheimer's disease and other CNS disorders (reviewed in [65]). Paradoxically, it was reported that HDAC1 and HDAC2 activity are required to regulate oligodendrocyte differentiation [66], and that HDAC1 and HDAC2 functions are critical for myelination and survival of Schwann cells in the peripheral nervous system [67]. These results do not necessarily negate the importance of HDAC1 and HDAC2 inhibition in mediating the effects seen in the present study, because of the different experimental conditions employed, namely, ischemic stroke in our study versus normal, non-pathological conditions in theirs. Future investigations exploring the role of specific isoform(s) involved in the pathophysiology of white matter injury and the beneficial effects of pan-HDAC inhibitors will provide crucial information for therapeutic interventions.

Acknowledgements

This study was supported by the Intramural Research Program of the National Institute of Mental Health, National Institutes of Health (IRP-NIMH-NIH). We are grateful to Dr. Carolyn Smith of NINDS, NIH for technical assistance with the confocal microscope study. We also thank Ioline Henter, Peter Leeds, and Zhifei Wang of the NIMH, NIH for editorial assistance.

Disclosure of conflict of interest

None.

Address correspondence to: Dr. De-Maw Chuang, Molecular Neurobiology Section, National Institute of Mental Health, National Institutes of Health, Building 10, Room 3D38, 10 Center Drive, MSC-

1363, Bethesda, MD 20892-1363, USA. Tel: 301-496-4915; Fax: 301-480-9290; E-mail: chuang@mail.nih.gov

References

[1] Fessler EB, Chibane FL, Wang Z, Chuang DM. Potential roles of HDAC inhibitors in mitigating ischemia-induced brain damage and facilitating endogenous regeneration and recovery. Curr Pharm Des 2013; 19: 5105-5120.

[2] Chuang DM, Leng Y, Marinova Z, Kim HJ, Chiu CT. Multiple roles of HDAC inhibition in neurodegenerative conditions. Trends Neurosci 2009; 32: 591-601.

[3] Chiu CT, Wang Z, Hunsberger JG, Chuang DM. Therapeutic Potential of Mood Stabilizers Lithium and Valproic Acid: Beyond Bipolar Disorder. Pharmacol Rev 2013; 65: 105-142.

[4] Wang Z, Fessler EB, Chuang DM. Beneficial effects of mood stabilizers lithium, valproate and lamotrigine in experimental stroke models. Acta Pharmacol Sin 2011; 32: 1433-1445.

[5] Ren M, Leng Y, Jeong M, Leeds PR, Chuang DM. Valproic acid reduces brain damage induced by transient focal cerebral ischemia in rats: potential roles of histone deacetylase inhibition and heat shock protein induction. J Neurochem 2004; 89: 1358-1367.

[6] Kim HJ, Rowe M, Ren M, Hong JS, Chen PS, Chuang DM. Histone deacetylase inhibitors exhibit anti-inflammatory and neuroprotective effects in a rat permanent ischemic model of stroke: multiple mechanisms of action. J Pharmacol Exp Thera 2007; 321: 892-901.

[7] Wang Z, Tsai LK, Munasinghe J, Leng Y, Fessler EB, Chibane F, Leeds P, Chuang DM. Chronic valproate treatment enhances postischemic angiogenesis and promotes functional recovery in a rat model of ischemic stroke. Stroke 2012; 43: 2430-2436.

[8] Wang Z, Leng Y, Tsai LK, Leeds P, Chuang DM. Valproic acid attenuates blood-brain barrier disruption in a rat model of transient focal cerebral ischemia: the roles of HDAC and MMP-9 inhibition. J Cereb Blood Flow Metab 2011; 31: 52-57.

[9] Kim HJ, Leeds P, Chuang DM. The HDAC inhibitor, sodium butyrate, stimulates neurogenesis in the ischemic brain. J. Neurochem 2009; 110: 1226-1240.

[10] Chari DM, Blakemore WF. New insights into remyelination failure in multiple sclerosis: implications for glial cell transplantation. Mult Scler 2002; 8: 271-277.

[11] Suzuki SO, Goldman JE. Multiple cell populations in the early postnatal subventricular zone take distinct migratory pathways: a dynamic study of glial and neuronal progenitor migration. J Neurosci 2003; 23: 4240-4250.

[12] Levison SW, Rothstein RP, Romanko MJ, Snyder MJ, Meyers RL, Vannucci SJ. Hypoxia/ischemia depletes the rat perinatal subventricular zone of oligodendrocyte progenitors and neural stem cells. Dev Neurosci 2001; 23: 234-247.

[13] Back SA, Han BH, Luo NL, Chricton CA, Xanthoudakis S, Tam J, Arvin KL, Holtzman DM. Selective vulnerability of late oligodendrocyte progenitors to hypoxia-ischemia. J Neurosci 2002; 22: 455-463.

[14] Jalal FY, Yang Y, Thompson J, Lopez AC, Rosenberg GA. Myelin loss associated with neuroinflammation in hypertensive rats. Stroke 2012; 43: 1115-1122.

[15] Káradóttir R, Cavelier P, Bergersen LH, Attwell D. NMDA receptors are expressed in oligodendrocytes and activated in ischaemia. Nature 2005; 438: 1162-1166.

[16] Salter MG, Fern R. NMDA receptors are expressed in developing oligodendrocyte processes and mediate injury. Nature 2005; 438: 1167-1171.

[17] Haynes RL, Baud O, Li J, Kinney HC, Volpe JJ, Folkerth DR. Oxidative and nitrative injury in periventricular leukomalacia. Brain Pathol 2005; 15: 225-233.

[18] Deng Y, Lu J, Sivakumar V, Ling EA, Kaur C. Amoeboid microglia in the periventricular white matter induce oligodendrocyte damage through expression of proinflammatory cytokines via MAP kinase signaling pathway in hypoxic neonatal rats. Brain Pathol 2008; 18: 387-400.

[19] Moxon-Emre I, Schlichter LC. Evolution of inflammation and white matter injury in a model of transient focal ischemia. J Neuropathol Exp Neurol 2010; 69: 1-15.

[20] Menn B, Garcia-Verdugo J, Yaschine C, Gonzalez-Perez O, Rowitch D, Alvarez-Buylla A. Origin of oligodendrocytes in the subventricular zone of the adult brain. J Neurosci 2006; 26: 7907-7918.

[21] Gonzalez-Perez O, Alvarez-Buylla A. Oligodendrogenesis in the subventricular zone and the role of epidermal growth factor. Brain Res Rev 2011; 67: 147-56.

[22] Kriegstein A, Alvarez-Buylla A. The glial nature of embryonic and adult neural stem cells. Annu Rev Neurosci 2009; 32: 149-184.

[23] Ming GI, Song HJ. Adult neurogenesis in the mammalian brain: significant answers and significant questions. Neuron 2011; 70: 687-702.

[24] Picard-Riera N, Decker L, Delarasse C, Goude K, Nait-Oumesmar B, Liblau R, Pham-Dinh D, Baron-Van Evercooren A. Experimental autoimmune encephalomyelitis mobilizes neural progenitors from the subventricular zone to un-

dergo oligodendrogenesis in adult mice. Proc Natl Acad Sci U S A 2002; 99: 13211-13216.
[25] McTigue DM, Horner PJ, Stokes BT, Gage FH. Neurotrophin-3 and brain-derived neurotrophic factor induce oligodendrocyte proliferation and myelination of regenerating axons in the contused adult rat spinal cord. J Neurosci 1998; 18: 5354-5365.
[26] Zhang JY, Luo XG, Xian CJ, Liu ZH, Zhou XF. Endogenous BDNF is required for myelination and regeneration of injured sciatic nerve in rodents. Eur J Neurosci 2000; 12: 4171-4180.
[27] Chan JR, Cosgaya, JM, Wu YJ, Shooter EM. Neurotrophins are key mediators of the myelination program in the peripheral nervous system. Proc Natl Acad Sci U S A 2001; 98: 14661-14668.
[28] Aria K, Lo EH. An oligovascular niche: cerebral endothelial cells promote the survival and proliferation of oligodendrocyte precursor cells. J Neurosci 2009; 29: 4351-4355.
[29] Miller MW, Nowakowski RS. Use of bromodeoxyuridine-immunohistochemistry to examine the proliferation, migration and time of origin of cells in the central nervous system. Brain Res 1988; 457: 44-52.
[30] Lee SR, Kim HY, Rogowska J, Zhao BQ, Bhide P, Parent JM, Lo EH. Involvement of matrix metalloproteinase in neuroblast cell migration from the subventricular zone after stroke. J Neurosci 2006; 26: 3491-3495.
[31] Xu J, Zhang QG, Li C, Zhang GY. Subtoxic N-methyl-D-aspartate delayed neuronal death in ischemic brain injury through TrkB receptor- and calmodulin-mediated PI-3K/Akt pathway activation. Hippocampus 2007; 17: 525-537.
[32] Back SA, Luo NL, Borenstein NS, Levine JM, Volpe JJ, Kinney HC. Late oligodendrocyte progenitors coincide with the developmental window of vulnerability for human perinatal white matter injury. J Neurosci 2001; 21: 1302-1312.
[33] Back SA, Han BH, Luo NL, Chricton CA, Xanthoudakis S, Tam J, Arvin KL, Holtzman DM. Selective vulnerability of late oligodendrocyte progenitors to hypoxia-ischemia. J Neurosci 2002; 22: 455-463.
[34] Sun Y, Jin K, Xie L, Childs J, Mao XO, Logvinova A, Greenberg DA. VEGF-induced neuroprotection, neurogenesis, and angiogenesis after focal cerebral ischemia. J Clin Invest 2003; 111: 1843-1851.
[35] Storkebaum E, Lambrechts D, Carmeliet P. VEGF: once regarded as a specific angiogenic factor, now implicated in neuroprotection. Bioessays 2004; 26: 943-954.
[36] Hermann DM, Zechariah A. Implications of vascular endothelial growth factor for postischemic neurovascular remodeling. J Cereb Blood Flow Metab 2009; 29: 1620-1643.
[37] Shimotake J, Derugin N, Wendland M, Vexler ZS, Ferriero DM. Vascular endothelial growth factor receptor-2 inhibition promotes cell death and limits endothelial cell proliferation in a neonatal rodent model of stroke. Stroke 2010; 41: 343-349.
[38] Nakamura K, Martin KC, Jackson JK, Beppu K, Woo CH, Thiele CJ. Brain-Derived Neurotrophic Factor Activation of TrkB Induces vascular endothelial growth factor expression via hypoxia-inducible factor-1a in neuroblastoma cells. Cancer Res 2006; 66: 4249-4255.
[39] Zheng Z, Yenari MA. Post-ischemic inflammation: molecular mechanisms and therapeutic implications. Neurol Res 2004; 26: 884-892.
[40] Chamorro A, Hallenbeck J. The harms and benefits of inflammatory and immune responses in vascular disease. Stroke 2006; 37: 291-293.
[41] Wang Q, Tang XN, Yenari MA. The inflammatory response in stroke. J Neuroimmuno 2007; 184: 53-68.
[42] Huang J, Upadhyay UM, Tamargo RJ. Inflammation in stroke and focal cerebral ischemia. Surg Neurol 2006; 66: 232-245.
[43] Lynch MA. The Multifaceted Profile of Activated Microglia. Mol Neurobiol 2009; 40: 139-156.
[44] Ladeby R, Wirenfeldt M, Garcia-Ovejero D, Fenger C, Dissing-Olesen L, Dalmau I, Finsen B. Microglial cell population dynamics in the injured adult central nervous system. Brain Res Brain Res Rev 2005; 48: 196-206.
[45] Broughton BRS, Reutens DC, Sobey CG. Apoptotic mechanisms after cerebral ischemia. Stroke 2009; 40: e331-339.
[46] Hyman BT, Yuan J. Apoptotic and non-apoptotic roles of caspases in neuronal physiology and pathophysiology. Nat Rev Neurosci 2012; 13: 395-406.
[47] Aguirre A, Dupree JL, Mangin JM, Gallo VA. Functional role for EGFR signaling in myelination and remyelination. Nat Neurosci 2007; 10: 990-1002.
[48] Gallo V, Armstrong RC. Myelin repair strategies: a cellular view. Curr Opin Neurol 2008; 3: 278-283.
[49] Liu XS, Chopp M, Kassis H, Jia LF, Hozeska-Solgot A, Zhang RL, Chen C, Cui YS, Zhang ZG. Valproic acid increases white matter repair and neurogenesis after stroke. Neuroscience 2012; 220: 313-321.
[50] Baltan S, Murphy SP, Danilov CA, Bachleda A, Morrison RS. Histone deacetylase inhibitors preserve white matter structure and function during ischemia by conserving ATP and reducing excitotoxicity. J Neurosci 2011; 31: 3990-3999.
[51] Baltan S, Murphy SP. Novel protective effects of histone deacetylase inhibition on stroke and

white matter ischemic injury. Neurotherapeutics 2013; 10: 798-807.
[52] Li J, Baud O, Vartanian T, Volpe JJ, Rosenberg PA. Peroxynitrite generated by inducible nitric oxide synthase and NADPH oxidase mediates microglial toxicity to oligodendrocytes. Proc Natl Acad Sci U S A 2005; 102: 9936-9941.
[53] Cho KO, La HO, Cho YJ, Sung KW, Kim SY. Minocycline attenuates white matter damage in a rat model of chronic cerebral hypoperfusion. J Neurosci Res 2006; 83: 285-291.
[54] Yenari MA, Liu J, Zheng Z, Vexler ZS, Lee JE, Giffard RG. Antiapoptotic and anti-inflammatory mechanisms of heat-shock protein protection. Ann N Y Acad Sci 2005; 1053: 74-83.
[55] Wang LW, Tu YF, Huang CC, Ho CJ. JNK signaling is the shared pathway linking neuroinflammation, blood-brain barrier disruption, and oligodendroglial apoptosis in the white matter injury of the immature brain. J Neuroinflammation 2012; 9: 1-17.
[56] Chiaramello S, Dalmasso G, Bezin L, Marcel D, Jourdan F, Peretto P, Fasolo A, De Marchis S. BDNF/TrkB interaction regulates migration of SVZ precursor cells via PI3-K and MAP-K signalling pathways. Eur J Neurosci 2007; 26: 1780-1790.
[57] Hung PL, Huang CC, Huang HM, Tu DG, Chang YC. Thyroxin treatment protects against white matter injury in the immature brain via brain-derived neurotrophic factor. Stroke 2013; 44: 2275-2283.
[58] Uluc K, Kendigelen P, Fidan E, Zhang L, Chanana V, Kintner D, Akture E, Song C, Ye K, Sun D, Ferrazzano P, Cengiz P. TrkB receptor agonist 7, 8 dihydroxyflavone triggers profound gender- dependent neuroprotection in mice after perinatal hypoxia and ischemia. CNS Neurol Disord Drug Targets 2013; 12: 360-370.
[59] Jin K, Zhu Y, Sun Y, Mao XO, Xie L, Greenberg DA. Vascular endothelial growth factor (VEGF) stimulates neurogenesis in vitro and in vivo. Proc Natl Acad Sci U S A 2002; 99: 11946-11950.
[60] Arai K, Lo EH. Experimental models for analysis of oligodendrocyte pathophysiology in stroke. Exp Transl Stroke Med 2009; 1: 1-8.
[61] Han BH, Holtzman DM. BDNF protects the neonatal brain from hypoxic-ischemic injury in vivo via the ERK pathway. J Neurosci 2000; 20: 5775-5781.
[62] Chen PS, Wang CC, Bortner CD, Peng GS, Wu X, Pang H, Lu RB, Gean PW, Chuang DM, Hong JS. Valproic acid and other histone deacetylase inhibitors induce microglial apoptosis and attenuate lipopolysaccharide-induced dopaminergic neurotoxicity. Neuroscience 2007; 149: 203-212.
[63] Fan W, Dai Y, Xu H, Zhu X, Cai P, Wang L, Sun C, Hu C, Zheng P, Zhao BQ. Caspase-3 modulates regenerative response after stroke. Stem Cells 2014; 32: 473-486.
[64] Lyssiotis CA, Walker J, Wu C, Kondo T, Schultz PG, Wu X. Inhibition of histone deacetylase activity induces developmental plasticity in oligodendrocyte precursor cells. Proc Natl Acad Sci U S A 2007; 104: 14982-14987.
[65] Chuang DM, Leng Y, Marinova Z, Kim HJ, Chiu CT. Multiple roles of HDAC inhibition in neurodegenerative conditions. Trends Neurosci 2009; 32: 591-601.
[66] Ye F, Chen Y, Hoang T, Montgomery RL, Zhao XH, Bu H, Hu T, Taketo MM, van Es JH, Clevers H, Hsieh J, Bassel-Duby R, Olson EN, Lu QR. HDAC1 and HDAC2 regulate oligodendrocyte differentiation by disrupting the beta-catenin-TCF interaction. Nat Neurosci 2009; 12: 829-838.
[67] Jacob C, Christen CN, Pereira JA, Somandin C, Baggiolini A, Lötscher P, Ozçelik M, Tricaud N, Meijer D, Yamaguchi T, Matthias P, Suter U. HDAC1 and HDAC2 control the transcriptional program of myelination and the survival of Schwann cells. Nat Neurosci 2011; 14: 429-436.